DØNote 4718 - v1.11 - CONF

Search for Neutral Supersymmetric Higgs Bosons in Multi–jet Events

The DØ Collaboration
URL: http://www-d0.fnal.gov

(Dated: February 23, 2005)

A search for the production of neutral Higgs bosons in association with bottom quarks is performed using 260 pb^{-1} of data collected with the DØ detector in Run II of the Fermilab Tevatron. The cross section of these processes may be enhanced in many extensions of the standard model such as the minimal super-symmetric extension of the standard model at large $\tan\beta$. The data agree well with standard model background estimations. Upper limits are set on the production rate of neutral Higgs bosons decaying to $b\overline{b}$ in the mass range of 90 to 150 GeV.

Preliminary Results for Winter 2005 Conferences

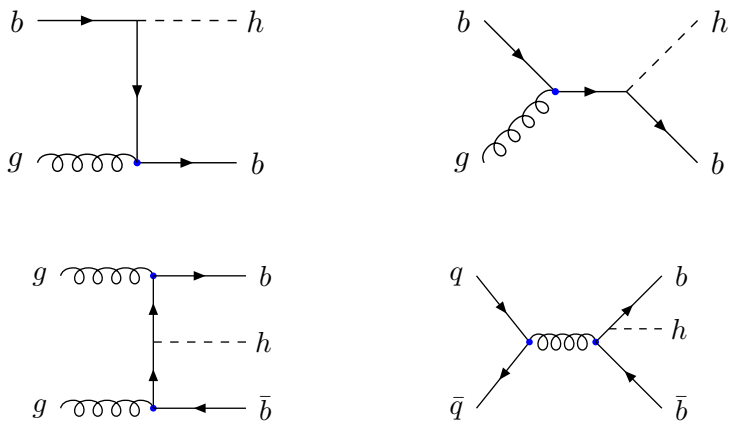

FIG. 1: Leading–order Feynman diagrams for neutral Higgs boson production in the five-flavor scheme (top) and four-flavor scheme (bottom).

I. INTRODUCTION

In two–Higgs–doublet models of electro-weak symmetry breaking, such as the minimal super-symmetric extension of the standard model (MSSM) [1], there are five physical Higgs bosons resulting from symmetry breaking: two neutral CP–even scalars, h and H, with H being the heavier state, a neutral CP–odd, A, and two charged states, $H^{\pm}$. The ratio of the vacuum expectation values of the two Higgs fields is defined as $\tan\beta = v_2/v_1$ where v_2 and v_1 refer to the fields which couple to the up- and down-type fermions, respectively. At tree level, the couplings of the neutral Higgs bosons to the down–type quarks, such as the bottom quark, are enhanced by a factor of $\tan\beta$ relative to the standard model (SM) predictions, thus production cross sections are enhanced by $\tan^2\beta$ [2], and branching fractions to $b\overline{b}$ by $\tan\beta$.

For most plausible scenarios of the MSSM, LEP experiments have excluded at 95% Confidence Level (C.L.) a light neutral Higgs boson, with $m_h < 92.9$ GeV [3]. At hadron colliders one can search for neutral Higgs boson production in association with b-quarks, in three or four b-jet final states. The CDF experiment at the Fermilab Tevatron performed such a search using Run I data at $\sqrt{s}$ =1.8 TeV [4].

Using data taken with the DØ detector from November 2002 – June 2004, corresponding to an integrated luminosity of about 260 pb^{-1}, we search for an excess of events in the di-jet invariant mass distribution of the two leading transverse momentum, p_T, jets in events containing three or more b-jets.

A. Higgs Bosons in the MSSM

Higgs boson production in association with b-quarks in $p\overline{p}$ collisions can be calculated in two ways: in the five-flavor scheme [5], only one b-quark needs to be present, while in the four–flavor scheme [6], two b-quarks are explicitly required in the final state. Figure 1 illustrates these processes at leading-order (LO). Similar diagrams exist for the H and the A. Both calculations are now available at next–to–leading order (NLO) and agree within their respective theoretical uncertainties [7, 8].

In this paper we assume CP conservation in the Higgs bosons sector. The masses, widths, and branching fractions for the neutral Higgs bosons are calculated using the CPsuperH program [9, 10]. The current analysis is sensitive to $\tan\beta$ in the region 50 – 100, depending on the Higgs boson mass. In this region of $\tan\beta$, the A is nearly degenerate in mass with either the h or the H, and their widths are small compared to the di–jet mass resolution of the detector. Consequently, one can not distinguish between the h/H or the A, and the total cross section is twice that of the A. The region of m_A from 100 – 130 GeV is of special interest since all three neutral Higgs bosons can be degenerate in mass and be produced simultaneously [11]. However, the total cross section still remains twice that of the A.

II. DATA AND MONTE CARLO SAMPLES

A. Trigger

Due to the high cross section of multi–jet events, a specialized trigger for the three trigger levels (L1, L2, L3) was designed to maximize signal acceptance while remaining within data acquisition constraints. The trigger demanded at least three calorimeter towers of size $\Delta\eta \times \Delta\phi = 0.2 \times 0.2$ at L1 where ϕ is the azimuthal angle, three jets and $H_T^{L2} > 50$ GeV at L2 ($H_T^{L2} \equiv$ scalar sum of the p_T of the L2 jets), and three jets with $p_T > 15$ GeV at L3.

B. Data Selection

A total of 87 million events were preselected with one reconstructed jet of $p_T > 20$ GeV and two more jets with $p_T > 15$ GeV, all with $|\eta| < 2.6$.

Jets are reconstructed using the cone algorithm [15] with radius of 0.5 and are then required to pass set of quality cuts. Jets with $p_T > 15$ GeV in $|\eta| < 2.5$ are considered. Their energies are corrected to the particle level using η–dependent scale factors. Events are preselected with at least three jets with corrected $p_T > 35$, 20, and 15 GeV, but not more than five jets. Depending on the Higgs boson mass, the final selection cuts are optimized for the signal significance defined as $S/\sqrt{B}$.

b-quark jets are identified using the Secondary Vertex (SV) tagging algorithm. A jet is tagged as a b-jet if it has at least one SV within $\Delta R = \sqrt{(\Delta\eta)^2 + (\Delta\phi)^2} < 0.5$ of the jet axis whose transverse displacement from the primary vertex exceeds five times its resolution. Jets are tagged up to $|\eta| < 2.5$, although the b-tagging is about twice as efficient in the central region ($|\eta| < 1.1$) because of the improved tracking resolution provided by the CFT. The $b$tagging efficiency is $\sim 35\%$ for central jets with $p_T > 35$ GeV, at a mis-tag rate of $\sim 2\%$.

C. Monte Carlo

Events of the expected signals and backgrounds were generated by PYTHIA [12] or ALPGEN [16] passed through PYTHIA showering. These events were then processed through the full DØ detector simulation and reconstruction chain. PYTHIA minimum–bias events were added to all generated events, Poisson distributed with a mean of 0.4 to simulate the instantaneous luminosities at which the data were taken ($1\text{–}6\times10^{31} cm^{-2}s^{-1}$).

1. Signal

bh events, with h decaying to $b\overline{b}$, were generated for different Higgs boson masses from 90 to 150 GeV. Reconstructed jets in simulated events were corrected to match the jet reconstruction and identification efficiency in data. The energy of simulated jets was smeared to match the measured jet energy resolution. The p_T and rapidity spectra of the Higgs bosons given by PYTHIA were compared to those from the NLO calculation [5]. The shapes were similar, indicating that the PYTHIA kinematics are approximately correct. To further improve the accuracy of the expectation, the simulated events were weighted to match the Higgs boson p_T spectrum given at NLO. There was a 10% reduction in the overall signal efficiency from this weighting.

2. Heavy–flavor Multi–jet

Of all standard model processes, multi–jet production is the major source of background. This background is determined from data, by normalizing outside the signal search region, but we also compared the observed multi–jet production with simulations as a cross-check. ALPGEN was used to generate events with final states of $b\overline{b}j$, $b\overline{b}jj$ with $j = u, d, s, c, g$, and $b\overline{b}b\overline{b}$ with generator–level cuts: $p_T^b > 25$ GeV, $p_T^j > 15$ GeV, $|\eta| < 3.0$, and $\Delta R > 0.4$ between any two jets. These generator level cuts do not introduce significant bias since the final sample (after trigger and b–tagging requirement) contains much harder jets. Cross sections obtained from ALPGEN were 8900 pb, 3900 pb, and 60 pb, respectively. The $b\overline{b}j$ and $b\overline{b}jj$ samples were added together, but the $b\overline{b}jj$ sample was weighted by 0.85 in order to match the jet multiplicity observed in double b-tagged data.

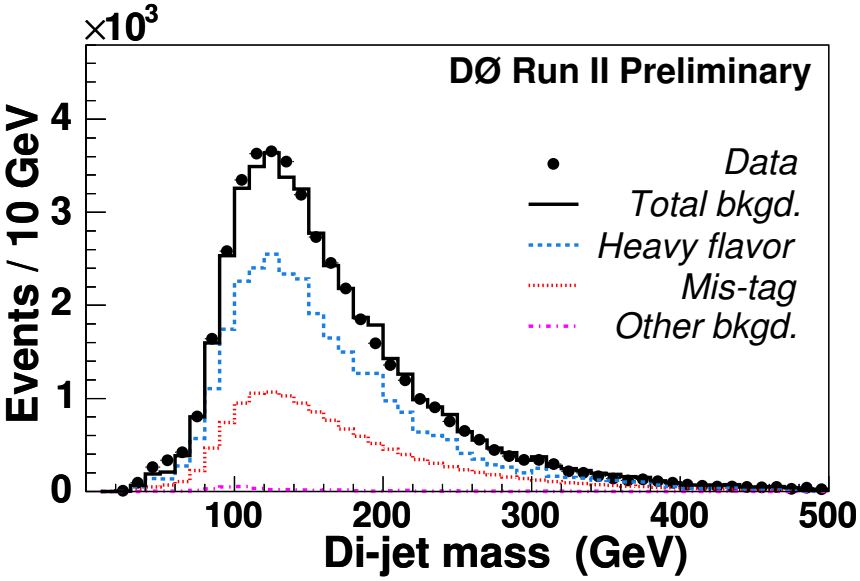

FIG. 2: Fit of the double b-tagged leading p_T di-jet invariant mass spectrum to a sum of backgrounds: Mis-tags derived from data, ALPGEN $b\bar{b}j(j)$ (dashed), and other small backgrounds ($Z(\rightarrow b\bar{b})$+jets, Zb, $t\bar{t}$ and ALPGEN $b\bar{b}b\bar{b}$) (dashed–dotted). The signal contribution to this sample is negligible.

3. *Other Backgrounds*

All other backgrounds are expected to be small and were simulated with PYTHIA as inclusive $p\bar{p}\rightarrow Z(\rightarrow b\bar{b})$+jets, $p\bar{p}\rightarrow Zb$, and $p\bar{p}\rightarrow t\bar{t}$. Cross sections of 1180 pb, 40 pb [17], and 7 pb were assumed, respectively.

III. ANALYSIS

A. Background Estimation

There are two main categories of multi–jet background: one contains genuine heavy–flavor (HF) jets, while the other has only light–quark or gluon jets which are tagged as b-quark jets by mistake, or possibly because the gluon jet branched into a nearly collinear $b\bar{b}$ pair. Using the preselected data sample before any b-tagging requirements, the probability to b-tag a jet is measured as a function of the p_T of the jet, in three different $|\eta|$ regions. These functions are called the "mis–tag" functions, although they are understood to have some contamination at this point from true HF events in the data sample from which they are derived. The mis–tag functions are corrected for this contribution, by estimating the fraction of $b\bar{b}j(j)$ events in the full multi–jet data sample (1.2%) from an initial fit to the double b-tagged data and subtracting the contribution from these events. These corrected mis–tag functions are then used to estimate the mis–tag background by applying them to every jet in the full data sample.

The double b-tagged multi–jet background is compared to simulations first, due to its high statistics. The expected signal contribution to the double b-tagged data is negligible. The comparison of the invariant mass spectrum of the highest two p_T jets in the double b-tagged data is shown in Fig. 2. The b-tagging used in this analysis is unable to distinguish contributions from bottom and charm events. However, the efficiency for tagging a charm–jet is known from simulations to be about 1/4 of that for tagging a b-jet. Therefore, when two b-tags are required, the fraction of $c\bar{c}j(j)$ events relative to $b\bar{b}j(j)$ events will be a factor of $\sim 4^2 = 16$ times lower after tagging than it was before. We have estimated the fractions of $c\bar{c}jj$ to $b\bar{b}jj$ prior to b-tagging using the MADGRAPH Monte Carlo generator [18]. The $c\bar{c}jj$ cross section was 22% higher than the $b\bar{b}jj$ one, using the same generator–level cuts. Therefore the contribution of $c\bar{c}j(j)$ in the double b-tagged data sample is expected to represent $\sim 1.22/16 = 8\%$ of the events. Thus, when we refer to the $b\bar{b}j(j)$ normalization, it should be understood that approximately 8% is from the $c\bar{c}j(j)$ process. After these corrections for $c\bar{c}j(j)$ events, the HF multi–jet processes are only a factor of 1.08 higher in data than predicted by ALPGEN. The data agree well with the shape of the estimated background over the entire invariant mass region.

To estimate the triple b-tagged background, the mis–tag function is applied to the non–b-tagged jets in the double b-tagged events. This provides the shape of the multi–jet background distribution with at least three b-tagged jets.

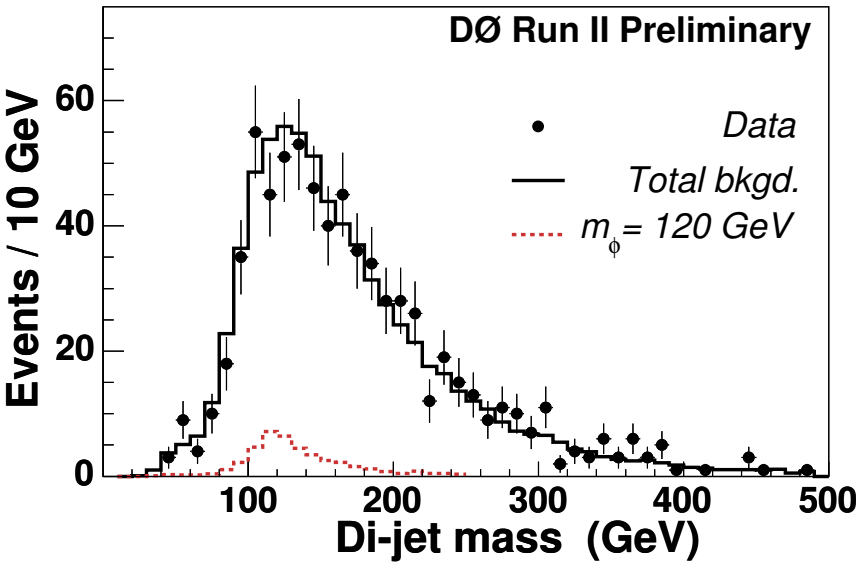

FIG. 3: The di-jet invariant mass spectrum of the triple b-tagged data, estimated background, and 120 GeV Higgs boson signal at the 95% C.L. exclusion limit.

Such a method neglects the contribution from processes which have more than two real b-jets, such as $b\bar{b}b\bar{b}$ and $Z(\rightarrow b\bar{b})b\bar{b}$. However, the shape of these backgrounds is seen to be similar in simulations to the double b-tagged spectrum, and their cross sections are small. The overall background normalization is determined by fitting the triple b-tagged invariant mass distribution outside the signal region ($\pm 1\sigma$ of the Gaussian fit to the expected signal) with the triple b-tag estimated shape.

B. Acceptance Systematics

The cuts made in this analysis take place in three sets: the trigger level, the kinematic cuts (p_T, η, n_j) where n_j is the number of jets, and b-tagging. Table I shows the acceptance of each set of cuts made in the analysis, for each m_A. Signal acceptance uncertainties are evaluated for various masses and are listed in Table II. Systematic errors resulting from the b-tagging efficiency, jet energy scale, jet energy resolution, and jet reconstruction/identification uncertainties are calculated by repeating the analysis, changing their values by $\pm 1\sigma$. In addition, the following uncertainties have small dependence on mass and are also added in quadrature: the procedure used to normalize the p_T distributions and cross sections of the simulated signal events to NLO, 5%; the integrated luminosity, 6.5%; and the trigger efficiency, 9%.

C. Background Systematics

The accuracy with which the shape of the background distribution is modeled can be estimated from the $\chi^2/d.o.f.$ of the background fit. The statistical error associated with the uncertainty in the normalization of the background, as fit outside the signal region, is multiplied by the $\sqrt{\chi^2/d.o.f.}$. The background uncertainty is estimated to be $\lesssim 3\%$. Another source of systematic uncertainty arises from the width of the signal search region used for the background normalization procedure. This uncertainty is evaluated by examining one more search window $\pm 1.8\sigma$. The resulting change in the background normalization is much smaller than the background uncertainty of 3%.

IV. RESULTS

The CL_S method, with $CL_S = CL_{S+B}/CL_B$, was used to set limits on signal production [19]. The full di–jet invariant mass distributions for the triple b-tagged events in data, simulated signal, and normalized background were used as inputs. The value of $\tan\beta$ was varied until the C.L. for signal was $< 5\%$. Figure 3 shows the data, background,

m_A (GeV)	Kinematic	Trigger	b-tag	Total
90	18	44	3.5	0.3
100	24	45	3.5	0.4
110	24	56	3.9	0.5
120	27	60	4.2	0.7
130	29	65	4.3	0.8
150	31	76	4.4	1.0

TABLE I: The acceptance for signal of each set of analysis cuts (in %).

m_A (GeV)	b-tag	Jet E. Scale	Jet E. Res.	Jet-ID	Total
90	14	7.5	1.4	3.8	20.4
100	15	7.1	0.7	3.8	21.0
110	14	8.1	0.7	3.7	20.6
120	14	8.5	0.8	3.6	21.0
130	14	7.8	0.4	3.3	20.4
150	15	7.7	0.8	3.4	21.1

TABLE II: The uncertainties from each source (in %). Other small uncertainties which do not depend on mass are also added in quadrature (see text).

and Higgs boson mass peak at the exclusion limit, for $m_A = 120$ GeV. This is converted to a cross section limit for signal production in Fig. 4, which also shows the expected MSSM Higgs boson production cross section as a function of m_A, for $\tan\beta = 80$. The NLO cross sections and their uncertainties due to parton distribution function (PDF) and scale variations are taken from [5, 8]. The enhancement factor of the cross section from the MSSM shown in Fig. 4 corresponds to the scenario with no mixing in the scalar top quark sector [20]: $X_t = 0$, where $X_t = A - \mu\ cot\beta$, with A being the tri–linear coupling, and μ – Higgsino mass parameter. We also interpret our results in maximal mixing scenario with $X_t = \sqrt{6} \times M_{SUSY}$, and M_{SUSY}, the mass scale of supersymmetric particles set at 1 TeV. Results for both scenarios are shown in Fig. 5 as limits on $\tan\beta$ versus m_A plane. The present DØ analysis, based on 260 pb^{-1}, excludes a significant portion of $\tan\beta$, down to 50, depending on m_A and the MSSM scenario assumed.

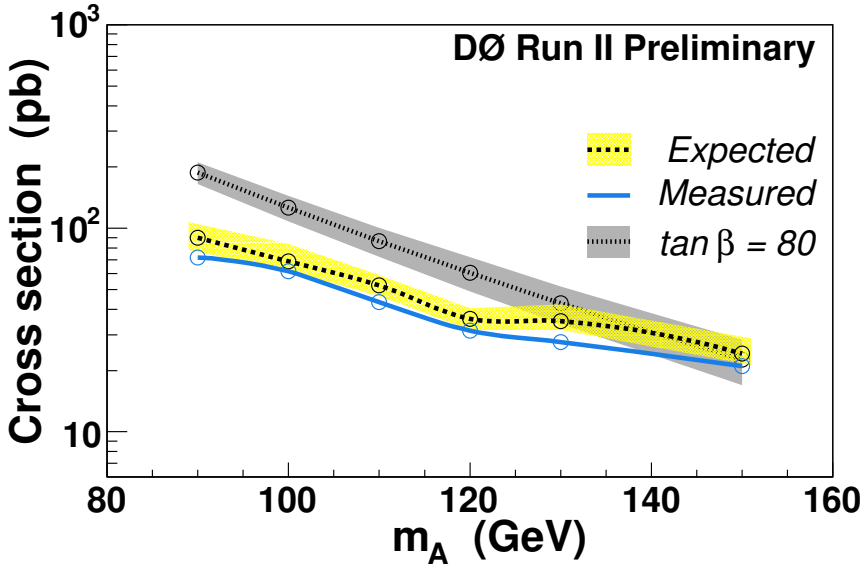

FIG. 4: The 95% C.L. expected and measured upper limits on signal production set as a function of m_A. The band indicates $\pm 1\sigma$ range on the expected limit. Also shown is the cross section for signal at $\tan\beta = 80$ in the "no mixing" scenario of the MSSM, with the theoretical uncertainty band overlayed.

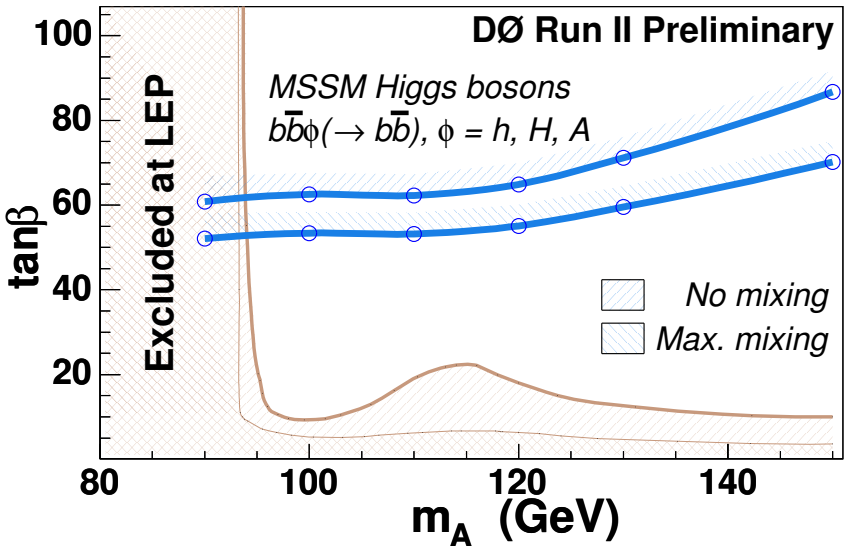

FIG. 5: The 95% C.L. upper limit on $\tan\beta$ set as a function of m_A for two scenarios of the MSSM, "no mixing" and "maximal mixing". Also shown are the limits obtained by LEP experiments [3].

Acknowledgments

We thank the authors of [5, 8, 20] for many hours of valuable discussions with us.

We thank the staffs at Fermilab and collaborating institutions, and acknowledge support from the Department of Energy and National Science Foundation (USA), Commissariat à l'Energie Atomique and CNRS/Institut National de Physique Nucléaire et de Physique des Particules (France), Ministry of Education and Science, Agency for Atomic Energy and RF President Grants Program (Russia), CAPES, CNPq, FAPERJ, FAPESP and FUNDUNESP (Brazil), Departments of Atomic Energy and Science and Technology (India), Colciencias (Colombia), CONACyT (Mexico), KRF (Korea), CONICET and UBACyT (Argentina), The Foundation for Fundamental Research on Matter (The Netherlands), PPARC (United Kingdom), Ministry of Education (Czech Republic), Canada Research Chairs Program, CFI, Natural Sciences and Engineering Research Council and WestGrid Project (Canada), BMBF and DFG (Germany), Science Foundation Ireland, A.P. Sloan Foundation, Research Corporation, Texas Advanced Research Program, Alexander von Humboldt Foundation, and the Marie Curie Fellowships.

[1] H. P. Nilles, Phys. Rept. **110**, 1 (1984); H. E. Haber and G. L. Kane, Phys. Rept. **117**, 75 (1985).
[2] J. F. Gunion, H. E. Haber, G. L. Kane and S. Dawson, "The Higgs Hunter's Guide,", SCIPP-89/13, 1989.
[3] LEP Higgs Working Group, LHWG-Note 2004-01.
[4] Recent theoretical calculations do not reproduce the cross sections and kinematics used by CDF Collaboration in Phys. Rev. Lett. **86**, 4472-4478 (2001). The result used PDFs which have been superseded, resulting in limits significantly more stringent than would have been obtained using the more recent PDFs used in this analysis.
[5] J. Campbell, R. K. Ellis, F. Maltoni and S. Willenbrock, Phys. Rev. D **67**, 095002 (2003).
[6] S. Dawson, C. B. Jackson, L. Reina and D. Wackeroth, Phys. Rev. D **69**, 074027 (2004); S. Dittmaier, M. Krämer and M. Spira, Phys. Rev. D **70**, 074010 (2004).
[7] J. Campbell *et al.*, hep-ph/0405302.
[8] S. Dawson, C. B. Jackson, L. Reina and D. Wackeroth, Phys. Rev. Lett.**94**, 031802 (2005).
[9] J. S. Lee *et al.*, Comp. Phys. Comm. **156**, 283 (2004).
[10] M. Carena and H. E. Haber, Prog. Part. Nucl. Phys. **50**, 63 (2003)
[11] E. Boos, A. Djouadi, M. Mühlleitner and A. Vologdin, Phys. Rev. D **66**, 055004 (2002).
[12] T. Sjöstrand *et al.*, Comp. Phys. Comm. **135**, 238 (2001).
[13] DØ Collaboration, V. Abazov *et al.*, in preparation for submission to Nucl. Instrum. Methods Phys. Res. A.
[14] DØ Collaboration, S. Abachi *et al.*, Nucl. Instrum. Methods Phys. Res. A **338**, 185 (1994).
[15] G. C. Blazey *et al.*, in *Proceedings of the Workshop: "QCD and Weak Boson Physics in Run II"*, edited by U. Baur, R. K. Ellis, and D. Zeppenfeld, Batavia, Illinois (2000) p. 47. See Section 3.5 for details.
[16] M. L. Mangano *et al.*, JHEP **0307**, 001 (2003).
[17] J. Campbell, R. K. Ellis, F. Maltoni and S. Willenbrock, Phys. Rev. D **69**, 074021 (2004).
[18] F. Maltoni and T. Stelzer, JHEP **0302**, 027 (2003).
[19] T. Junk, Nucl. Instrum. Methods Phys. Res., Sect. A **434** 435 (1999).
[20] M. Carena, S. Mrenna and C. E. M. Wagner, Phys. Rev. D **60**, 075010 (1999); Phys. Rev. D **62**, 055008 (2000).